

Density Functional Theory Investigation of the Alkyl–Alkyl Negishi Cross-Coupling Reaction Catalyzed by N-Heterocyclic Carbene (NHC)–Pd Complexes

**Gregory A. Chass,*^[a] Christopher J. O'Brien,^[b] Niloufar Hadei,^[b]
Eric Assen B. Kantchev,^[b] Wei-Hua Mu,^[c] De-Cai Fang,*^[c] Alan C. Hopkinson,^[b]
Imre G. Csizmadia,^[d] and Michael G. Organ*^[b]**

Abstract: A novel mechanism is proposed for the Pd–1,3-(2,6-diisopropylphenyl)imidazolyl-2-ylidene (**1**) catalyzed Negishi reaction. DFT computations supported by atoms-in-molecules (AIM) analyses of non-truncated models show that a “steric wall” created by the *N*-substituent on the ligand guides reactants to and from the Pd

center. Notably, transmetalation and not oxidative addition is found to be rate-limiting. Additionally, a key Pd–Zn interaction ($\approx 2.4 \text{ \AA}$, $\rho_b \approx 0.0600 \text{ au}$)

Keywords: cross-coupling • density functional calculations • N-heterocyclic carbenes • palladium • zinc

is identified in the mechanism. This interaction persists beyond reductive elimination and, in combination with the ligand, facilitates reductive elimination by creating a highly sterically crowded environment in the coordination sphere of the Pd center.

Transition-metal-catalyzed cross-coupling reactions^[1] for the construction of carbon–carbon and carbon–heteroatom bonds have had a profound effect in organic synthesis. Pd-based catalysts^[2,3] provide convenient routes allowing the synthetic chemist to access a vast array of complex molecules, drugs, and materials. Even though a number of cross-

coupling reactions of relatively simple substrates can be performed successfully in high yields with various forms of elemental Pd,^[4] soluble Pd complexes with organic ligands such as tertiary phosphanes^[1,3,5] or N-heterocyclic carbenes (NHCs)^[6] are necessary for more challenging substrate combinations. The traditional mechanism^[1] (Scheme 1) of Pd-mediated cross-coupling reactions involves three *discrete*

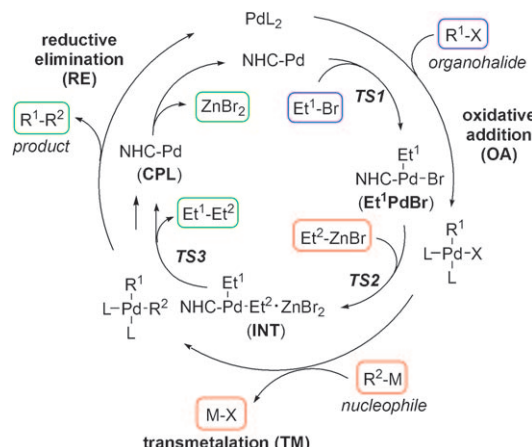
[a] Dr. G. A. Chass
School of Chemistry, University of Wales
Bangor, LL57 2UW (UK)
Fax: (+44) 1248-370528
E-mail: gchass@giocomms.org

[b] Dr. C. J. O'Brien, Dr. N. Hadei, Dr. E. A. B. Kantchev,
Prof. A. C. Hopkinson, Prof. M. G. Organ
Department of Chemistry, York University
4700 Keele Street, Toronto, ON, M3J 1P3 (Canada)
Fax: (+1) 416-736-5936
E-mail: organ@yorku.ca

[c] W.-H. Mu, Prof. D.-C. Fang
College of Chemistry, Beijing Normal University
Beijing, 100875 (China)
Fax: (+86) 10-58805422
E-mail: dcfang@bnu.edu.cn

[d] Prof. I. G. Csizmadia
Department of Chemistry,
University of Toronto, ON, M5G 2E8 (Canada)

Supporting information for this article is available on the WWW under <http://dx.doi.org/10.1002/chem.200900042>.



Scheme 1. The generally accepted mechanism for the Pd-mediated cross-couplings (outer circle) and the mechanism for alkyl–alkyl Negishi cross-coupling as calculated in this work (inner circle).

steps: 1) *oxidative addition* (OA): insertion of Pd⁰ into the carbon–halide bond with Pd⁰ being oxidized to Pd^{II}; 2) *transmetalation* (TM): transfer of the second carbon fragment to Pd^{II} from an organometallic compound concomitant with inorganic salt formation, which dissociates from the complex; 3) *reductive elimination* (RE): expulsion of the product hydrocarbon with regeneration of the Pd⁰ catalyst.

The importance of Pd-mediated cross-coupling has led to numerous computational studies that have revealed important insights into the structure and behavior of NHC–Pd^[7–9] and phosphane–Pd^[10,11] catalysts and actual or putative catalytic cycle intermediates as well as the nature of oxidative addition,^[11–13] transmetalation,^[14] and reductive elimination^[15] steps. Computational analysis of whole catalytic cycles^[9,16] have been performed much less frequently. In silico studies also have been used occasionally for ligand design.^[8,17]

Cross-couplings of alkyl substrates are considered to be particularly challenging due to retardation of both oxidative addition and reductive elimination (compared to the unsaturated systems), in addition to the existence of a major competing pathway, β -hydride elimination that would lead to products resembling **5** and **6**, for instance, in Table 1.^[18] Recently, we discovered that Pd ligated by a bulky NHC, 1,3-bis(2,6-diisopropylphenyl)imidazol-2-ylidene (IPr) (**1**) (Table 1), prepared either *in situ*^[19,20] or from a well-defined complex^[21,22] efficiently catalyzes the alkyl–alkyl Negishi cross-coupling of alkylbromides and chlorides possessing β -hydrogen atoms at room temperature.

A less sterically hindered carbene, (1,3-bis(2,6-dimethylphenyl)imidazol-2-ylidene) (IXy) (Pd–IXy, **2**)^[14] leads to predominantly β -hydride elimination (e.g., **5**). Although there are computational studies of oxidative addition of alkyl halides to Pd,^[12] there are no computational studies on either the complete cycle of any Pd-mediated alkyl–alkyl coupling or Pd-mediated Negishi reaction.^[14f] Aiming to fill this important void, we present herein a density functional theory (DFT) in silico examination of the NHC–Pd-mediated alkyl–alkyl Negishi reaction (Table 1 and Scheme 1) at the B3LYP^[23]/DZVP (a DFT-optimized all-electron basis set

with double-zeta valence+polarization)^[24] level of theory. Through-space interactions and bond formation/breaking were also studied by atoms-in-molecules (AIM) electron density topological analyses.^[25] We^[20,21] and others^[26] have demonstrated that the steric bulk of the flanking N-substituents has an immense effect on the reaction (Table 1). To link computation and experiment, herein we present calculations of the complete sp³–sp³ cross-coupling cycles (Figure 1) catalyzed by Pd ligated with IPr (Pd–IPr, **1**) or IXy (Pd–IXy, **2**)^[27] in solution employing the polarizable continuum model (PCM)^[28] method with THF as the solvent ($\epsilon=7.58$, 298 K).^[29] All structures were confirmed as residing at minima or first-order saddle points on their respective potential energy hypersurfaces (PEHSs). Structures, transition states and pathways that failed to optimize were re-attempted multiple times using different geometries, retaining/relaxing coordinates and other techniques to eliminate computational artifacts.

This study finds that whereas the general mechanism is followed (Scheme 1), introducing the bulky NHC ligand causes significant differences. In the active catalyst, a mono-ligated NHC–Pd complex (Figure 2),^[20,27,30] the NHC ligand occupies one of the six Pd-coordination trajectories. The *ortho*-alkyl substituents force the phenyl rings perpendicular to the NHC-ring plane, creating a “steric wall” that differentiates the remaining five trajectories as “side” (two), “top” (two), and “front” with respect to the Pd–NHC bond as it lies in the plane of the NHC ring, with “top” and “side” approaches being more sterically hindered than “front”. Besides the expected (NHC)C2–Pd interaction, AIM analysis revealed four weak ($\rho_b=0.004$ au each) agostic iPr–H–Pd interactions from each of the isopropyl groups in **1**, shown on the two-dimensional Laplacian (Figure 2b, gray circles) for the electronic density of the NHC-bound Pd atom taken in the plane of the Pd–NHC bond (Figure 2a, blue). The only NHC–Pd interaction in **2** is with the carbene carbon (C2, Figure 2c). Such weak interactions were also observed throughout the whole catalytic cycle (Figure 3, green dashed lines) for **1**, but not for **2**.

Importantly, whereas $\Delta H^{\ddagger 0}$ ₂₉₈ and ΔH^0 ₂₉₈ values are very close for both NHCs in every step of the cycle (Figure 1), **1** has a higher entropy contribution ($-T\Delta S^0$) arising from low-energy motions of the iPr substituents. These motions permit up to 4 out of the 24 methyl hydrogen atoms from the iPr group to form weak interactions with Pd. These interactions appear and disappear during the various stationary points in the cycle, and they appear to coordinatively saturate Pd. These interactions change the energetic landscape of the process, destabilizing intermediates more than transition states, “something that makes for a better cross-coupling cycle”.^[10b] Whereas **2** yielded products arising from cross-coupling (**4**; 0.7%), β -hydride elimination (**5** and **6**; 78.0% total), and reduction (**7**; 21.3%), the use of **1** resulted in quantitative cross-coupling (Table 1). It should also be noted that control experiments performed with PdCl₂, or with no catalyst at all, resulted in a quantitative recovery of **3**. These experiments confirm that both catalysts oxidatively

Table 1. The Negishi alkyl–alkyl cross-coupling reaction mediated by mono-ligated NHC–Pd complexes (calibrated GC–MS yields). Model substrates used in silico are shown for comparison.

NHC	Ar	4 [%]	5+6 [%]	7 [%]
IPr (1)	2,6-iPr ₂ Ph	100.0	0	0
IXy (2)	2,6-Me ₂ Ph	0.7	78.0	21.3

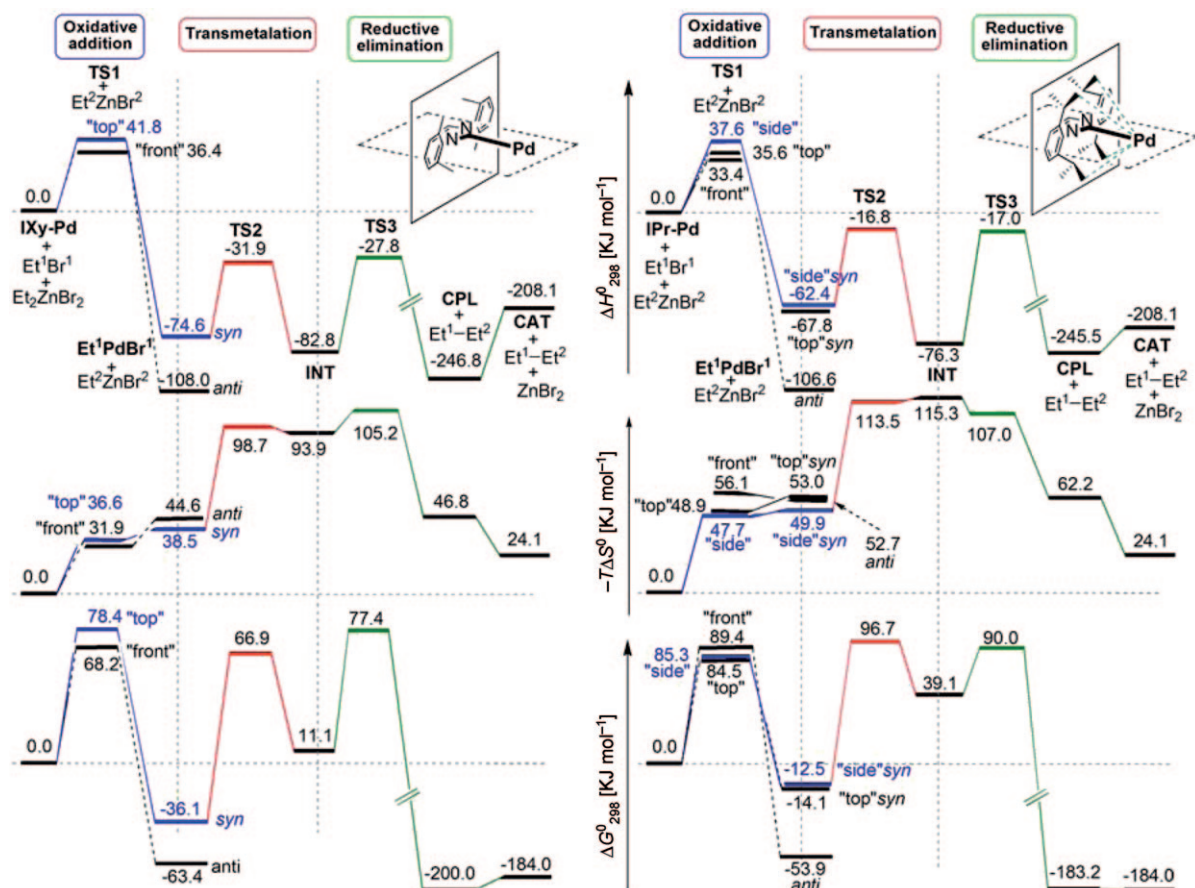


Figure 1. Relative enthalpy (ΔH^0_{298}), entropy ($T\Delta S^0$) at 298 K and free-energy (ΔG^0_{298}) values (kJ mol^{-1}) calculated at the B3LYP/DZVP level, for the alkyl–alkyl cross-coupling reaction (Scheme 1) mediated by IPr-Pd (1, right) and a less sterically hindered analogue, IXy-Pd (2, left).

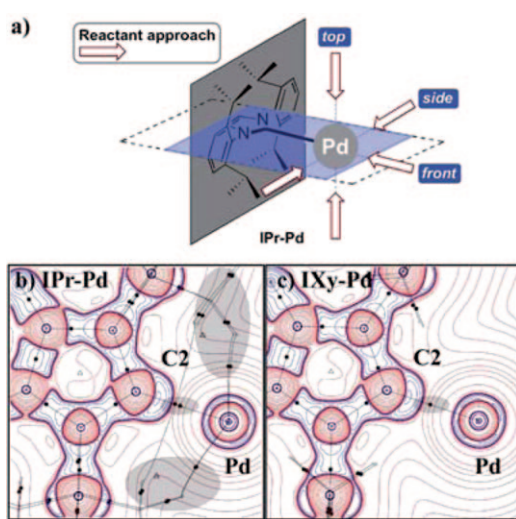


Figure 2. a) Reactant approaches to IPr-Pd (1) from “side”, “top”, and “front” directions with respect to IPr-Pd bond lying in the plane of the NHC ring. 2D-Laplacians generated from the wavefunctions of the B3LYP/DZVP-optimized IPr-Pd (1, b) and IXy-Pd (2, c) structures taken in the plane of NHC-Pd bond (a), blue plane. Interactions identified by AIM analyses are shaded in gray.

insert very effectively, so oxidative addition is not rate-limiting for either one of them. This can be observed experimentally as the reactions with both catalysts produce a noticeable exotherm. While the origin of this ligand chemoselectivity is not completely clear, we hypothesize that the weak (*iPr*)H–Pd interactions aid in suppressing β -hydride elimination through coordinatively saturating Pd.

Nowhere is the entropic effect of the weak (*iPr*)H–Pd interactions more apparent than during oxidative addition, where the entropy contribution originating from IPr stabilizes the transition state for the “syn” approach and destabilizes the resulting intermediate, effectively avoiding the “anti-trap” that befalls catalyst 2 (vide infra). During oxidative addition, the alkyl bromide approaches Pd following “front”, “top”, or “side” trajectories (Figure 3, TS1) forming a three-center transition state comprising of Pd, Br, and the α -carbon of Et¹. “Top” and “side” approaches lead to two conformers of the “syn”-oxidative addition intermediate (9 and 11; Figure 4). *syn* and *anti* are defined by the (NHC)C₂-Pd-Br¹ bond angle values of $\approx 90^\circ$ and $\approx 180^\circ$, respectively. The (Et¹)C₂-Pd-Br¹ angle is always $\approx 90^\circ$. Dihedral angles for Br¹-Pd-C₂(NHC)-N1/3(NHC) are $-2.2^\circ/176^\circ$ and $-85^\circ/100^\circ$ in “top” *syn* and “side” *syn* conformers, respectively. For IPr-Pd (1), these conformers interconvert with very low

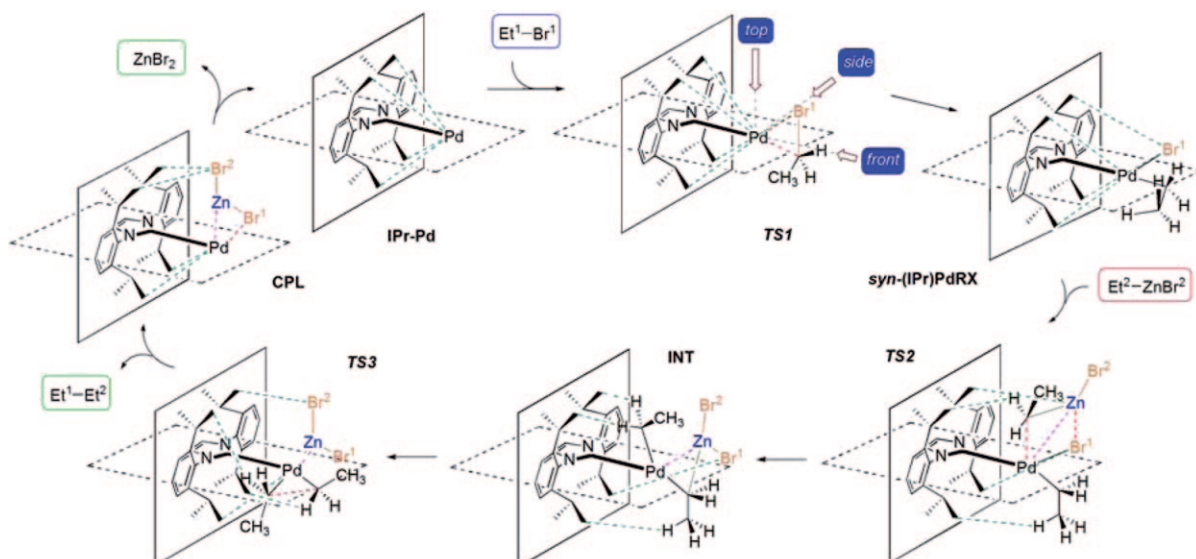


Figure 3. Optimized structures calculated at B3LYP/DZVP level of theory for the alkyl–alkyl Negishi cross-coupling reaction (Scheme 1) mediated by IPr–Pd (**1**). Weak guiding (iPr)H–Pd interactions are shown (green dashed lines).

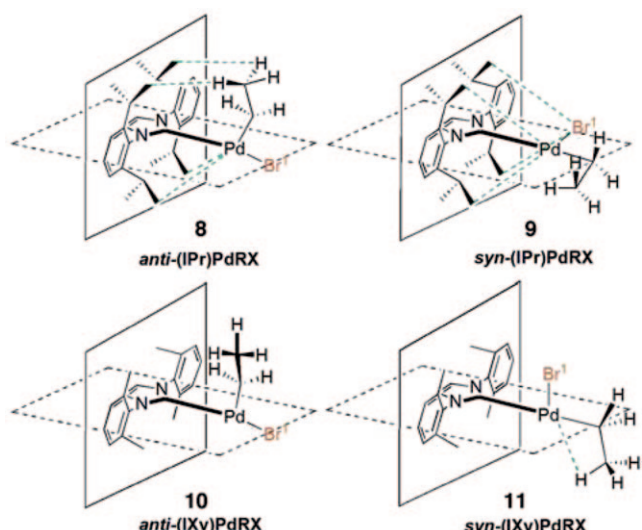


Figure 4. Optimized structures for the oxidative addition intermediates (for detailed description see text) calculated at B3LYP/DZVP level of theory. For IPr (**1**), only the “side” syn-conformer is shown for simplicity. Selected weak (iPr)H–Pd interactions are shown (green dashed lines).

barriers via rotation of the Pd–C2(NHC) bond ($\Delta G^{\ddagger 0}_{298}=4.0$ and 5.6 kJ mol^{-1} , for “side→top” and “top→side”, respectively), and therefore are considered as one (**9**). Surprisingly, for catalyst **2**, “side” approach resulted in a large increase of energy, and the corresponding oxidative addition intermediate conformation and transition state both failed to optimize, suggesting a non-homogeneous boundary shape for **2** (not shown). Therefore, only the “top” approach leads to syn-oxidative addition intermediate (**11**). Importantly, the “front”-approach (leading to the anti-oxidative intermediate **10**) has a *higher* barrier than the “side” and “top” approaches ($\Delta G^{\ddagger 0}_{298}=89.4$ versus 85.3 kJ mol^{-1}) for **1**, but

lower than “top” (“side” being unavailable) for **2** ($\Delta G^{\ddagger}=68.2$ versus 78.4 kJ mol^{-1}). anti-Oxidative addition intermediates (**8** and **10**) are the most energetically favorable for both NHC ligands due to Coulombic repulsion between the NHC and Br¹ ($\Delta G^0_{298}=-53.9$ and $-63.4 \text{ kJ mol}^{-1}$ for **1** and **2**, respectively, Figure 1). Interestingly, our repeated attempts at finding a transmetalation transition state starting from the anti-PdRX intermediate for both **1** and **2** failed due to a rapid increase in energy resulting from the steric clash between the incoming, Zn-bound Et² fragment and the NHC ligand in the associative transmetalation transition state. As for **2**, the anti-intermediate is both more stable and forms more easily; the oxidative addition intermediate becomes effectively “trapped” in the anti-configuration. For **1**, the syn-adduct resulting from “side” approach (**9**), forms faster than the anti-adduct (**8**, $\Delta G^{\ddagger 0}_{298}=85.3$ versus 89.4 kJ mol^{-1}) and is the least stable ($\Delta G^0_{298}=-12.5$ versus $-53.9 \text{ kJ mol}^{-1}$); therefore, it is being most activated for transmetalation in a catalytic cycle that is under kinetic control.

Transmetalation from the syn-PdRX intermediate had the highest free energy of activation ($\Delta G^{\ddagger 0}_{298}=103.0$ and $109.2 \text{ kJ mol}^{-1}$ for **2** and **1**, respectively), becoming the rate-determining step for the catalytic cycle of both catalysts (Figure 1). Geometrically, in TS2 for **1**, Et² is being transferred to Pd at the vacant “top” position, whereas Br¹ is starting to bond to Zn from its “syn” position (Figure 5a). AIM analyses also provided evidence for this in the form of additional, unexpected interactions between Zn and Pd ($\rho_b=0.033 \text{ au}$, 2.725 \AA) and iPr(H)-Et²(H) ($\rho_b=0.006 \text{ au}$, 2.347 \AA) that help to guide the organozinc partner into position. In INT, BCPs show both Pd and Zn to be three-coordinate (Figure 5b). The Pd–Zn interaction is broken in **1** due to steric crowding in the highly entropically disfavored INT structure ($+115.3 \text{ kJ mol}^{-1}$ contribution from entropy), lead-

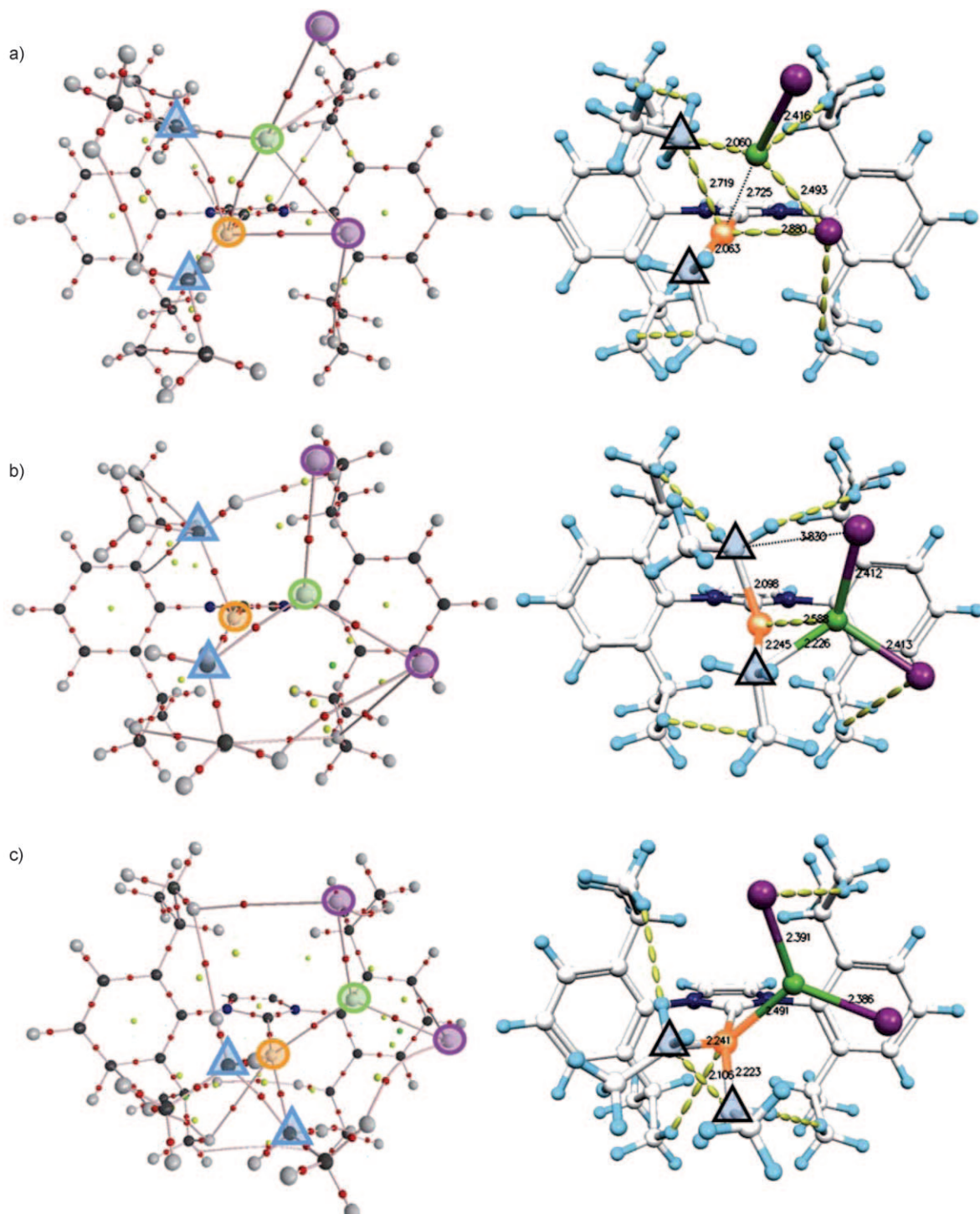


Figure 5. Molecular graphs of the wavefunctions (left) and structures (right) of the B3LYP/DZVP geometry-optimized TS2 (a), INT (b), TS3 (c) for iPr-Pd (1). Orange, green, and purple spheres highlight Pd, Zn, and Br atoms, respectively. Blue triangles highlight the C atoms of Et¹ and Et² that interact with Pd. Bond and ring critical points are shown in red and yellow, respectively. Dashed yellow lines show weak interactions identified by AIM analyses.

ing to temporary loss of all weak (*i*Pr)H–Pd interactions as well. By comparison, in the less crowded **2**, Pd–Zn strengthens ($\rho_b=0.046$ au, 2.547 Å) retaining the TS2-like geometry. In TS3 (Figure 5c), Et² moves away from “top” and pulls Et¹ outwards and away from the Zn atom, which now re-

enters the coordination sphere of Pd ($\rho_b=0.053$ au, 2.491 Å). TS3 is less crowded, and *i*Pr-H-Pd interactions appear again to assist in pushing away the product molecule. The presence of ZnBr₂ in the coordination sphere of the Pd atom during and beyond the reductive elimination provides

additional steric interactions that may aid the expulsion of the cross-coupling product, contrary to the accepted mechanism (Scheme 1), which requires ZnBr_2 to dissociate prior to commencement of reductive elimination, and suggests that these processes may not be discrete steps. The Pd-Zn interaction ($\rho_b=0.059 \text{ au}$, 2.426 \AA and $\rho_b=0.058 \text{ au}$, 2.438 \AA , for **2** and **1**, respectively) persists even after the departure of the cross-coupling product. The adduct between the highly electron-rich NHC-Pd⁰ and the Lewis acidic ZnBr_2 is observed as an additional intermediate in the cycle (CPL).^[31]

In conclusion, the first computational study of the complete catalytic cycle for the Pd-mediated alkyl-alkyl Negishi reaction revealed that the bulky NHC ligands introduce important differences into the traditionally accepted mechanism. First, transmetalation and not oxidative addition, which is considered to be slow in comparison with that for aryl halides,^[18] was found to be the rate-determining step for the whole cycle. Second, the inorganic salt by-product (ZnBr_2) was found not to dissociate prior to reductive elimination, as suggested in the traditional mechanism. This increased steric crowding during transmetalation helps to release the product (*n*-butane). The complex between the highly electron-rich IPr-Pd⁰ and the Lewis acidic ZnBr_2 persisted even after the cross-coupled product was formed. Third, four (*i*Pr)H atoms from the two *N*-(2,6-diisopropylphenyl) substituents in **1** were found to form fleeting weak interactions with Pd that appeared and disappeared during the various stages of the cycle, depending on the steric crowding around Pd. We propose that these interactions facilitate the molecular mechanism that results in the high activity of IPr-ligated **1**. They change the free energy landscape through increasing the entropy term ($-T\Delta S^0$) in the free energy, destabilizing intermediates more than transition states, leading to higher turnover frequency and coordinatively saturate Pd throughout the cycle. Although the exact molecular mechanism by which the structure of the IPr ligand helps steer the course of the reaction to cross-coupling or β -hydride elimination remains unsolved at this time, this study has shed light on some of the ligand effects governing the product ratio resulting from the two competing pathways. Finally, it is important to note that the use of truncated computational models, for example, using the dimethylimidazolium analogue of diarylimidazolium-based **1**, failed to reveal any of the aforementioned subtle interactions between the isopropyl substituents of the NHC ligand and the reacting metal center that are responsible, and in fact critical for directing **1** down a productive path in the catalytic cycle.^[32]

Experimental Section

Cross-coupling experiments: The following cross-coupling protocol was used for both catalyst **1** (Pd-PEPPSI-IPr) and **2** (Pd-PEPPSI-IXy). In air, a vial was charged with Pd-PEPPSI-IPr (3.4 mg) or Pd-PEPPSI-IXy (3.0 mg) (1 mol %) and under an inert atmosphere, LiBr (139.0 mg, 1.6 mmol), and a stir bar were added. The vial was then sealed with a septum and purged with argon after which THF (1.6 mL) was added and

the suspension was stirred until the solids dissolved. After this time, *n*-butylzinc bromide (0.8 mL, 1.0 M in DMI, 0.8 mmol) and 3-phenyl-1-bromo-propane (**3**) (0.5 mmol) were added. The septum was replaced with a Teflon-lined screw cap under an inert atmosphere and the reaction was stirred for 2 h at room temperature. After this time, GC/MS analysis was conducted by removing a 2 μL aliquot of the reaction mixture and diluting with distilled hexane (1 mL). The resulting solution was then filtered through a plug of celite and analyzed. GCMS analysis of product ratios was conducted (in triplicate) on a Varian Series GC/MS/MS 4000 System using undecane as an internal standard. The above experiment (for each catalyst system) was conducted twice and the averaged yield is reported in Table 1. The spectra obtained for products **4–7** were consistent with that reported in the literature.^[22]

Computational methods: The Gaussian 03 (G03) program package^[33] was used for all computations in this work. Analytical frequencies were computed on the geometry-optimized structures to ensure the identity of each structure as residing at minima or first-order saddle points on the PEHSs of the systems. Zero-point energy (ZPE) and the thermodynamic parameters required to quantify the free energy (ΔG) of each structure were also extracted from these frequency evaluations.

An established numeric and modular description of all molecular structures was used in the generation of inputs for geometry optimizations.^[34] This allowed for novel Perl and shell-based UNIX/Linux scripting to be continuously built-up and refined, to facilitate file construction, job submission, data storage/extraction, tabulation and automation. Accurate *in silico* determinations are highly dependent upon accurate initial starting structures.

Geometry optimizations were carried out with density functional theory (DFT) using the B3LYP^[23a,c] method, employing the DZVP basis set^[24] with a self-consistent reaction field polar continuum (solvent) model (SCRF-PCM = THF).^[28a–c]

In regard to the atoms-in-molecules (AIM) approach, critical points (CPs) of rank 3 were identified in the electron densities; these include bond critical points (BCPs), ring critical points (RCPs), and cage critical points (CCPs). The existence of a BCP between two atoms in an equilibrium molecular geometry is the necessary condition for two atoms to be defined as being bound to one another. The pairs of gradient paths that originate at a BCP and terminate at neighboring nuclei, define a line through which electron distribution, $\rho(r)$, is a maximum with respect to any lateral displacement.

B3LYP/DZVP wavefunctions, generated with G03, were used to obtain molecular graphs and BCP properties using the AIM2000 program.^[35,36]

Acknowledgments

We thank GIOCOMMS and Project 985 (China) for computational support, ORDCF (Ontario, Canada), NSERC (Canada), CAFMaD (Wales, UK), and the National Natural Sciences Foundation of China (20773016) for funding.

- [1] *Metal-catalyzed cross-coupling reactions*, 2nd ed. (Eds.: A. De Meijere, F. Diederich), Wiley, New York, **2004**.
- [2] K. C. Nicolaou, P. G. Bulger, D. Sarlah, *Angew. Chem.* **2005**, *117*, 4516–4563; *Angew. Chem. Int. Ed.* **2005**, *44*, 4442–4482#4489#.
- [3] *Handbook of Organopalladium Chemistry for Organic Synthesis* (Ed.: E. Negishi), Wiley, New York, **2002**.
- [4] V. Farina, *Adv. Synth. Catal.* **2004**, *346*, 1553–1582.
- [5] a) C. C. Mauger, G. A. Mignani, *Aldrichimica Acta* **2006**, *39*, 17–24; b) A. Zapf, M. Beller, *Chem. Commun.* **2005**, 431–440.
- [6] a) *N-Heterocyclic Carbenes in Transition Metal Catalysis* (Ed.: F. Glorius), Springer, Heidelberg, **2007**; b) E. A. B. Kanchev, C. J. O'Brien, M. G. Organ, *Angew. Chem.* **2007**, *119*, 2824–2870; *Angew. Chem. Int. Ed.* **2007**, *46*, 2768–2813. c) *N-Heterocyclic Carbenes in Synthesis* (Ed.: S. P. Nolan), Wiley-VCH, Weinheim, **2006**; d) W. A.

- Herrmann, *Angew. Chem.* **2002**, *114*, 1342–1363; *Angew. Chem. Int. Ed.* **2002**, *41*, 1290–1309.
- [7] a) B. V. Popp, J. E. Wendlandt, C. R. Landis, S. S. Stahl, *Angew. Chem.* **2007**, *119*, 607–610; *Angew. Chem. Int. Ed.* **2007**, *46*, 601–604; b) V. Lillo, E. Mas-Marza, A. M. Segarra, J. J. Carbó, C. Bo, E. Peris, E. Fernandez, *Chem. Commun.* **2007**, 3380–3382; c) B. V. Popp, S. S. Stahl, *J. Am. Chem. Soc.* **2007**, *129*, 4410–4422; d) E. F. Penka, C. W. Schlapfer, M. Atanasov, M. Albrecht, C. Daul, *J. Organomet. Chem.* **2007**, *692*, 5709–5716; e) R. J. Nielsen, W. A. Goddard III, *J. Am. Chem. Soc.* **2006**, *128*, 9651–9660; f) C. J. O'Brien, E. A. B. Kantchev, G. A. Chass, N. Hadei, A. C. Hopkinson, M. G. Organ, D. H. Setiadi, T.-H. Tang, D.-C. Fang, *Tetrahedron* **2005**, *61*, 9723–9735; g) K. Albert, P. Gisdakis, N. Rosch, *Organometallics* **1998**, *17*, 1608–1616.
- [8] D. V. Yandulov, N. T. Tran, *J. Am. Chem. Soc.* **2007**, *129*, 1342–1358.
- [9] a) M.-T. Lee, H. M. Lee, C.-H. Hu, *Organometallics* **2007**, *26*, 1317–1324; b) J. C. Green, B. J. Herbert, R. Lonsdale, *J. Organomet. Chem.* **2005**, *690*, 6054–6067.
- [10] a) T. Ikawa, T. E. Barder, M. R. Biscoe, S. L. Buchwald, *J. Am. Chem. Soc.* **2007**, *129*, 13001–13007; b) S. Kozuch, C. Amatore, A. Jutand, S. Shaik, *Organometallics* **2005**, *24*, 2319–2330; c) J. P. Stambuli, M. Bühl, J. F. Hartwig, *J. Am. Chem. Soc.* **2002**, *124*, 9346–9347.
- [11] a) L. J. Goossen, D. Koley, H. L. Herrmann, W. Thiel, *Organometallics* **2006**, *25*, 54–67; b) J. P. Stambuli, C. D. Incarvito, M. Bühl, J. F. Hartwig, *J. Am. Chem. Soc.* **2004**, *126*, 1184–1194; c) L. J. Goossen, D. Koley, H. L. Herrmann, W. Thiel, *Chem. Commun.* **2004**, 2141–3143; d) M. H. Pérez-Temparano, A. Nova, J. A. Casares, P. Espinet, *J. Am. Chem. Soc.* **2008**, *130*, 10518–10520.
- [12] For computational studies of oxidative addition of alkyl halides, see: a) A. Ariafard, Z.-Y. Lin, *Organometallics* **2006**, *25*, 4030–4033; b) A. Diefenbach, F. M. Bickelhaupt, *J. Chem. Phys.* **2001**, *115*, 4030–4040. For studies of oxidative addition to allyl chlorides, see: c) H. Kurosawa, H. Kajimaru, S. Ogoshi, H. Yoneda, K. Miki, N. Kasai, S. Murai, I. Ikeda, *J. Am. Chem. Soc.* **1992**, *114*, 8417–8424; d) H. Kurosawa, S. Ogoshi, Y. Kawasaki, S. Murai, M. Miyoshi, I. Ikeda, *J. Am. Chem. Soc.* **1990**, *112*, 2813–2814.
- [13] a) P.-O. Norrby, M. Ahlquist, *Organometallics* **2007**, *26*, 550–553; b) R. Fazaeli, A. Ariafard, S. Jamshidi, E. S. Tabatabaei, K. A. Pishro, *J. Organomet. Chem.* **2007**, *692*, 3984–3993; c) T. E. Barder, M. R. Biscoe, S. L. Buchwald, *Organometallics* **2007**, *26*, 2183–2192; d) M. Ahlquist, P. Fristrup, D. Tanner, P.-O. Norrby, *Organometallics* **2006**, *25*, 2066–2073; e) L. J. Goossen, D. Koley, H. L. Herrmann, W. Thiel, *Organometallics* **2005**, *24*, 2398–2410; f) H. M. Senn, T. Ziegler, *Organometallics* **2004**, *23*, 2980–2988.
- [14] a) R. Álvarez, O. N. Faza, A. R. De Lera, D. J. Cárdenas, *Adv. Synth. Catal.* **2007**, *349*, 887–906; b) A. A. C. Braga, N. H. Morgan, G. Ujaque, A. Lledos, F. Maseras, *J. Organomet. Chem.* **2006**, *691*, 4459–4466; c) A. A. C. Braga, N. H. Morgan, G. Ujaque, F. Maseras, *J. Am. Chem. Soc.* **2005**, *127*, 9298–9307; d) E. Napolitano, V. Farina, M. Persico, *Organometallics* **2003**, *22*, 4030–4037; e) A. Nova, G. Ujaque, F. Maseras, A. Lledos, P. Espinet, *J. Am. Chem. Soc.* **2006**, *128*, 14571–14578; f) For a recent mechanistic study on transmetalation in the Negishi reaction, see: J. A. Casares, P. Espinet, B. Fuentes, G. Salas, *J. Am. Chem. Soc.* **2007**, *129*, 3508–3509.
- [15] a) V. P. Ananikov, D. G. Musaev, K. Morokuma, *Organometallics* **2005**, *24*, 715–723; b) E. Zuidema, P. W. N. M. van Leeuwen, C. Bo, *Organometallics* **2005**, *24*, 3703–3710; c) V. P. Ananikov, D. G. Musaev, K. Morokuma, *J. Am. Chem. Soc.* **2002**, *124*, 2839–2852.
- [16] a) P. Surawatanawong, Y.-B. Fan, M. B. Hall, *J. Organomet. Chem.* **2008**, *693*, 1552–1563; b) T. E. Barder, S. L. Buchwald, *J. Am. Chem. Soc.* **2007**, *129*, 12003–12010; c) S. Kozuch, S. Shaik, *J. Am. Chem. Soc.* **2006**, *128*, 3355–3365; d) A. A. C. Braga, G. Ujaque, F. Maseras, *Organometallics* **2006**, *25*, 3647–3658; e) R. Álvarez, O. N. Faza, C. S. López, A. R. De Lera, *Org. Lett.* **2006**, *8*, 35–38; f) L. J. Goossen, D. Koley, H. L. Herrmann, W. Thiel, *J. Am. Chem. Soc.* **2005**, *127*, 11102–11114; g) T. R. Cundari, J. Deng, *J. Phys. Org. Chem.* **2005**, *18*, 417–425.
- [17] a) N. Fey, J. N. Harvey, G. C. Lloyd-Jones, A. G. Orpen, R. Osborne, M. Purdie, *Organometallics* **2008**, *27*, 1372–1383; b) I. J. S. Fairlamb, A. F. Lee, *Organometallics* **2007**, *26*, 4087–4089; c) C. Thoumazet, H. Grützmacher, B. Deschamps, L. Ricard, P. le Floch, *Eur. J. Inorg. Chem.* **2006**, 3911–3922.
- [18] a) A. C. Frisch, M. Beller, *Angew. Chem.* **2005**, *117*, 680–695; *Angew. Chem. Int. Ed.* **2005**, *44*, 674–688; b) D. J. Cárdenas, *Angew. Chem.* **2003**, *115*, 398–401; *Angew. Chem. Int. Ed.* **2003**, *42*, 384–387; c) T.-Y. Luh, M.-K. Leung, K.-T. Wong, *Chem. Rev.* **2000**, *100*, 3187–3204.
- [19] N. Hadei, E. A. B. Kantchev, C. J. O'Brien, M. G. Organ, *Org. Lett.* **2005**, *7*, 3805–3807.
- [20] N. Hadei, E. A. B. Kantchev, C. J. O'Brien, M. G. Organ, *J. Org. Chem.* **2005**, *70*, 8503–8507.
- [21] C. J. O'Brien, E. A. B. Kantchev, C. Valente, N. Hadei, G. A. Chass, A. Lough, A. C. Hopkinson, M. G. Organ, *Chem. Eur. J.* **2006**, *12*, 4743–4748.
- [22] M. G. Organ, S. Avola, I. Dubovyk, N. Hadei, E. A. B. Kantchev, C. J. O'Brien, C. Valente, *Chem. Eur. J.* **2006**, *12*, 4749–4755.
- [23] For B3LYP DFT functional see: a) A. D. Becke, *J. Chem. Phys.* **1993**, *98*, 5648–5652; b) B. Mehlrich, A. Savin, H. Stoll, H. Preuss, *Chem. Phys. Lett.* **1989**, *157*, 200–206; c) C. Lee, W. Yang, R. G. Parr, *Phys. Rev. B* **1988**, *37*, 785–789.
- [24] N. Godbout, D. R. Salahub, J. Andzelm, E. Wimmer, *Can. J. Chem.* **1992**, *70*, 560–571.
- [25] a) R. F. W. Bader, D.-C. Fang, *J. Chem. Theory Comput.* **2005**, *1*, 403–414; b) R. F. W. Bader, *Atoms in Molecules: a Quantum Theory*, Clarendon Press, Oxford, **1990**.
- [26] J. Zhou, G. C. Fu, *J. Am. Chem. Soc.* **2003**, *125*, 12527–12530.
- [27] G. A. Grasa, M. S. Viciu, J. Huang, C. Zhang, M. L. Trudell, S. P. Nolan, *Organometallics* **2002**, *21*, 2866–2873.
- [28] a) V. Barone, M. Cossi, *J. Phys. Chem. A* **1998**, *102*, 1995–2001; b) V. Barone, M. Cossi, J. Tomasi, *J. Chem. Phys.* **1997**, *107*, 3210–3221; c) S. Miertus, E. Scrocco, J. Tomasi, *J. Chem. Phys.* **1981**, *74*, 75, 117–129.
- [29] Tests with one explicit THF molecule bound to the Pd through O (*anti*, Figure 1) in both perpendicular and co-planar arrangement relative to the NHC-ring plane showed that the dissociation energy of the THF was 24.2 and 38.1 kJ mol⁻¹ for *i*Xy-Pd (**2**) and *i*Pr-Pd (**1**), respectively, with the latter structure being a first-order saddle point, force constants showing the solvating THF molecule moving away from NHC-Pd. Similarly, computations with one explicit THF molecule fixed with the O-atom positioned at 2.40 Å from Zn in [(*i*Pr)Pd(ZnBr₂)] (CPL) and subsequently geometry-optimized showed no change in the geometric structure of CPL with Zn remaining bound to Pd and THF having moved to 2.11 Å relative to Zn (first-order saddle point), with a net ΔG_{298}^0 difference of +20.84 kJ mol⁻¹, relative to the unbound state. These ΔG_{298}^0 values are smaller than the reaction barriers (Figure 1), removing concern that implicit models may miss competitive inhibition of reaction by solvating particles.
- [30] a) L.-C. Campeau, P. Thansandote, K. Fagnou, *Org. Lett.* **2005**, *7*, 1857–1860; b) H. Lebel, M. K. Janes, A. B. Charette, S. P. Nolan, *J. Am. Chem. Soc.* **2004**, *126*, 5046–5047; c) M. S. Viciu, R. F. Germaineau, O. Navarro-Fernandez, E. D. Stevens, S. P. Nolan, *Organometallics* **2002**, *21*, 5470–5472.
- [31] a) While this work was in progress, a similar Pd–Zn interaction was computationally derived: R. Álvarez, A. R. De Lera, J. M. Aurrecochea, A. Durana, *Organometallics* **2007**, *26*, 2799–2802; b) For similar Ni–Zn interaction see: H. P. Hratchian, S. K. Chowdhury, V. M. Gutierrez-Garcia, K. K. D. Amarasinghe, M. J. Heeg, H. B. Schlegel, J. Montgomery, *Organometallics* **2004**, *23*, 4636–4646.
- [32] M. G. Organ, G. A. Chass, D.-C. Fang, A. C. Hopkinson, C. Valente, *Synthesis* **2008**, 2776–2797.
- [33] B3LYP/DZVP wavefunctions, generated with G03, were used to obtain molecular graphs and BCP properties using AIM2000 program. Gaussian 03, Revision B02, M. J. Frisch, G. W. Trucks, H. B. Schlegel, G. E. Scuseria, M. A. Robb, J. R. Cheeseman, J. A. Montgomery Jr., T. Vreven Jr., K. N. Kudin, J. C. Burant, J. M. Millam,

S. S. Iyengar, J. Tomasi, V. Barone, B. Mennucci, M. Cossi, G. Scalmani, N. Rega, G. A. Petersson, H. Nakatsuji, M. Hada, M. Ehara, K. Toyota, R. Fukuda, J. Hasegawa, M. Ishida, T. Nakajima, Y. Honda, O. Kitao, H. Nakai, M. Klene, X. Li, J. E. Knox, H. P. Hratchian, J. B. Cross, C. Adamo, J. Jaramillo, R. Gomperts, R. E. Stratmann, O. Yazyev, A. J. Austin, R. Cammi, C. Pomelli, J. W. Ochterski, P. Y. Ayala, K. Morokuma, G. A. Voth, P. Salvador, J. J. Dannenberg, V. G. Zakrzewski, S. Dapprich, A. D. Daniels, M. C. Strain, O. Farkas, D. K. Malick, A. D. Rabuck, K. Raghavachari, J. B. Foresman, J. V. Ortiz, Q. Cui, A. G. Baboul, S. Clifford, J. Cioslowski, B. B. Stefanov, G. Liu, A. Liashenko, P. Piskorz, I. Komaromi, R. L. Martin, D. J. Fox, T. Keith, M. A. Al-Laham, C. Y. Peng,

A. Nanayakkara, M. Challacombe, P. M. W. Gill, B. Johnson, W. Chen, M. W. Wong, C. Gonzalez, J. A. Pople, Gaussian, Inc., Pittsburgh PA, **2003**.

- [34] G. A. Chass, M. A. Sahai, J. M. S. Law, S. Lovas, O. Farkas, A. Perczel, J. L. Rivail, I. G. Csizmadia, *Int. J. Quantum Chem.* **2002**, *90*, 933–968.
[35] F. Biegler-König, J. Schonbohm, D. Bayles, *J. Comput. Chem.* **2001**, *22*, 545.
[36] F. Biegler-König, J. Schonbohm, *J. Comput. Chem.* **2002**, *23*, 1489.

Received: January 7, 2009

Published online: March 13, 2009